Circadian rhythmicity of the thioredoxin system in cultured murine peritoneal macrophages

D Couchie, T Medali, V Diderot, M Raymondjean, B Friguet, M Rouis

Biochimie 198 (2022) 76–85

Contents lists available at ScienceDirect

Biochimie

journal homepage: www.elsevier.com/locate/biochi

Circadian rhythmicity of the thioredoxin system in cultured murine peritoneal macrophages

D. Couchie, T. Medali, V. Diderot, M. Raymondjean, B. Friguet, M. Rouis*

Sorbonne Université, CNRS, INSERM, Institut de Biologie Paris Seine, Biological Adaptation and Ageing (B2A-IBPS), F-75005, Paris, France

ARTICLE INFO

Article history:
Received 25 January 2022
Received in revised form
15 March 2022
Accepted 22 March 2022
Available online 25 March 2022

Keywords:
Circadian rhythm
Circadian clocks
Clock genes
Thioredoxin
Thioredoxin-interacting protein
Oxidative stress
Pathophysiology
Vascular biology
Macrophages

ABSTRACT

Macrophages play a pivotal role in atherosclerosis through a variety of events related to cellular oxidative stress. This process is mainly due to an excessive production of reactive oxygen species whose elimination occurs through antioxidant systems including the thioredoxin (Trx) system. In this paper, we investigated whether the Trx system would exhibit circadian rhythmicity in dexamethasone synchronized cultured macrophages and monitored the impact of the rhythmicity of Trx-1 on markers of atherosclerosis. We found that the clock-related genes *BMAL-1*, *PER-2*, *CRY-1* and *REV ERB* α exhibited a robust circadian expression. However, the Trx genes family (*Trx-1, Trx-2, TrxR1 and TXNIP*) did not exhibit a circadian expression at the mRNA level in spite of the presence of E-box elements within the promoter regions of *TrxR1* and *TXNIP* genes. Nevertheless, both Trx-1 and TXNIP exhibited a circadian expression at the protein level and proteasome inhibition abolished the rhythmicity of Trx-1. Moreover, we found a link between low Trx-1 level and elevated atherogenic markers such as 4-HNE, TNF-α and cholesterol accumulation in macrophages. Our results indicate that the Trx gene family does not exhibit the same circadian regulation and that the presence of E-box elements in the *TXNIP* promoter is not sufficient to ensure a circadian rhythmicity at the transcriptional level. In addition, since a link was found between a low level of Trx-1 protein during circadian rhythm and high levels of atherogenic markers, administration of Trx-1 at certain time points could be an interesting approach to protect against atherosclerosis development.

1. Introduction

Atherosclerosis, a complex disease process, involves the interaction of several cells within the vessel wall (*e.g.* smooth muscle cells, endothelial cells and monocytes/macrophages). Macrophages play an important role in the disease development, essentially *via* the accumulation of oxidized low-density lipoprotein (oxLDL) [1], and the secretion of inflammatory mediators, cytokines, and extracellular matrix-degrading enzymes [2]. The majority of these events are linked to cellular oxidative stress, due mainly to the reactive oxygen species (ROS) which affect transcriptional regulation of a number of genes through redox-sensitive transcription factors [3].

ROS are highly reactive molecules and their levels are determined by a balance between their production and their elimination. The principal site of ROS production in the cell is the mitochondrial respiratory chain but other important sources exist such as NADPH oxidase, cyclooxygenases, peroxisomal enzymes, and the cytochrome P450 system. Their elimination can be observed through the antioxidant systems among which superoxide dismutases, catalases, peroxiredoxins, glutaredoxins, glutathione and the thioredoxin (Trx) system (reviewed in Ref. [4]). Excessive production of ROS results in oxidative stress which plays a major role in the pathogenesis of several human diseases, including atherosclerosis [5].

It has been shown that acute myocardial infarction is the principal cause of death in patient with atherosclerotic disease [6,7]. Yet, the underlying mechanisms are not completely understood. Nevertheless, the circadian clock and clock genes may play a role in this process. A 24 h periodicity has led to the evolution of molecular circadian clocks in various organisms from cyanobacteria to humans. In mammals the suprachiasmatic in hypothalamic has been found to be the master pacemaker controlling circadian rhythm in physiology [8]. Peripheral organs (*e.g*; liver, heart, kidney,

* Corresponding author. CNRS-SU UMR 8256/INSERM U1164, Sorbonne Université, 7 Quai Saint Bernard, 75252, Paris Cedex 5, France.
E-mail address: mustapha.rouis@sorbonne-universite.fr (M. Rouis).

https://doi.org/10.1016/j.biochi.2022.03.006

Abbreviations

Thioredoxin-1 (Trx-1)
Thioredoxin-2 (Trx-2)
Thioredoxin Reductase-1 (TrxR1)
Thioredoxin-Interacting Protein (TXNIP)
4-hydroxynonenal (4-HNE)
Tumor Necrosis Factor (TNF-α)
Oxidized Low-Density Lipoprotein (oxLDL)
Reactive Oxygen Species (ROS)
Period Proteins (PER-1, PER-2, and PER-3)
Cryptochrome proteins (CRY-1 and CRY-2)
CCGs (Clock Controlled genes)
Dexamethasone (DEX)

skin) and cells in culture also contain circadian oscillators. The circadian clock is constituted of positive and negative transcriptional feedback loops. The core feedback loops of the mammalian molecular clock include three period proteins (PER-1, PER-2, and PER-3), two cryptochrome proteins (CRY-1 and CRY-2), CLOCK, NPAS2 and two BMAL (BMAL-1 and BMAL-2) proteins. In mammals, CLOCK and BMAL-1 form a heterodimer and bind to CACGTG or CACGTT type E-box elements, which are located in the promoters of *PER* and *CRY* genes and induce their transcription [9,10]. The PER and CRY proteins form a complex which inhibits CLOCK/BMAL-1-mediated transcription of *PER* and *CRY* genes leading to the formation of the core negative feedback loop. In addition, REV ERB α is under the control of CLOCK/BMAL-1 heterodimer. The REV ERB α protein represses *BMAL-1* transcription, thus, inducing the oscillation of *BMAL-1* gene expression. The CLOCK/BMAL-1 activates y the transcription of *PER* or *CRY* genes and many other genes, called clock controlled genes (CCGs).

The generation of ROS may arise from daily variations in metabolism controlled by the circadian clock. Thus, daily and circadian oscillations of pro- and antioxidant enzymes and low-molecular weight molecules have been documented [11]. Among antioxidants, the Trx system was reported to be a very important system in plants and has been shown to be under circadian control. In contrast, its regulation by the circadian clock in mammals is not well known [12]. In this study, we have investigated whether Trx system would exhibit circadian rhythmicity in synchronized cultured mice peritoneal macrophages, one of the principal cellular components in atherosclerosis development. Of note, Trx-1, Trx-2, Thioredoxin Reductase-1 (TrxR1) and Thioredoxin-interacting protein (TXNIP), the endogenous Trx-1 inhibitor, have been collectively referred as to the Trx system [13–16]. Three forms of mammalian Trx, encoded by separate genes have been reported: cytosolic Trx (Trx-1), mitochondrial Trx (Trx-2), and a Trx (SpTrx or Trx-3) that has been reported to be highly expressed in spermatozoa [17–19]. In this manuscript, the SpTrx/Trx-3 has not been studied.

2. Materials and Methods

2.1. Reagents and culture medium

RPMI 1640 medium, Dulbecco's Modified Eagle's Medium, fetal bovine serum, L-glutamine, penicillin and streptomycin were purchased from Gibco LifeTechnologies. Expression plasmids containing the coding region of *mBMAL-1*, *mCLOCK* and *mDBP* were generously provided by Kazuhiro Yagita (Kyoto Prefectural University of Medicine, Kyoto, Japan).

2.2. Isolation and dexamethasone or serum shock treatment of murine peritoneal macrophages

Peritoneal macrophages were collected from thioglycolate-injected 12-week-old C57Bl/6 mice (Janvier Labs) by peritoneal lavage with 10 ml phosphate-buffered saline and centrifuged at 1000 rpm for 10 min. Cells were cultured in RPMI 1640 medium containing 10% (v/v) heat-inactivated fetal bovine serum (FBS), 2 mM L-glutamine, 100 U/ml penicillin and 100 μg/ml streptomycin in a humidified 5% CO_2 incubator at 37 °C. at 90% of confluence, circadian synchronization of cells was performed by a shock treatment that consists in a 2 h exposure to a 100 nM dexamethasone (DEX) (Sigma-Aldrich) or a serum-rich (RPMI 1640 supplemented by 50% of horse serum) treatment. The cells were then placed in a serum free culture medium. The time 0 (t_{0h}) corresponds to the beginning of the DEX shock. Then every 4 h and for 52 h, cells were harvested and RNA or protein extractions were performed.

All procedures involving animal handling and their care were in accordance with the Sorbonne Université Guidelines for Husbandry of Laboratory Mice.

2.3. Quantitative reverse Transcription-PCR analysis

Total RNA was extracted from synchronized macrophages using the RNeasy Plus Mini Kit (Qiagen). Reverse transcription was realized using the RevertAid H Minus First Strand cDNA Synthesis Kit (ThermoScientific) with random hexamers. Real time qPCR analysis was performed on a LightCycler 480 with the Go Taq qPCR Master Mix (Promega) using a SYBR Green I dye for product detection. Primer sequences used in PCR reactions are listed in Table 1. Relative quantification of target RNA using *36B4* as reference was realized with the $\Delta\Delta C_T$ method.

2.4. Cloning of mTXNIP promoter reporters

Two 5′ flanking regions of the *mTXNIP* gene (GenBank accession no. AF282825) were amplified by PCR from mouse liver genomic DNA. A 1213-bp fragment, including four E-box-like elements and a 484-bp fragment including two E-box-like elements, corresponding respectively to the region (−1214/-2) and (−485/-2) of the *mTXNIP* promoter were produced using the forward primers: 5′-TGG CCT AAC TGG CC (14 bp extension homologous to vector end) *GGTACC* (*Kpn I*) CCA CCT CTT GTT TCC TGG AGA AA-3′ or 5′-TGG CCT

Table 1
Mouse sequences of primers used for qPCR analysis.

Genes	Primers
36B4	Forwards 5′- AGC TGA AGC AAA GGA AGA GTC GGA -3′
	Reverse 5′- ACT TGG TTG CTT TGG CGG GAT TAG -3′
BMAL-1	Forwards 5′- AAG CTT CTG CAC AAT CCA CAG CAC -3′
	Reverse 5′- TGT CTG GCT CAT TGT CTT CGT CCA -3′
CRY-1	Forwards 5′- AGA ATG TCC CGA GTT GTA GCA GCA -3′
	Reverse 5′- AGC TTC TCC CTT GCT TGA GTG AGT -3′
PER-2	Forwards 5′- TTC CTA CAG CAT GGA GCA GGT TGA -3′
	Reverse 5′- ATG AGG AGC CAG GAA CTC CAC AAA -3′
REV ERB α	Forwards 5′- ACC TTA CTG CTC AGT GCC TGG AAT -3′
	Reverse 5′- TGG ACC TTG ACA CAA ACT GGA GGT -3′
Trx-1	Forwards 5′- AAG CTT GTC GTG GTG GAC TTC TCT -3′
	Reverse 5′- AAC TGG AAG GTC GGC ATG CAT TTG -3′
Trx-2	Forwards 5′- ACA TTT CCT CTC CTG CCT CTG CTT -3′
	Reverse 5′- TGG GCT CTG TTC TTC ACA GCA AGA -3′
TrxR1	Forwards 5′- AGT GGC GTT TCA CAG TAC CCT TCT -3′
	Reverse 5′- ACA GTC AAC TCC CTT GGT TTC CCT -3′
TXNIP	Forwards 5′- AAG CTG TCC TCA GTC AGA GGC AAT -3′
	Reverse 5′- ATG ACT TTC TTG GAG CCA GGG ACA -3′

AAC TGG CC (14 bp extension homologous to vector end) *GGTACC* (*Kpn I*) CGC ACC CGA ACA ACA ACC AT-3′ and reverse primer: 5′-TAT CCT CGA G (10 bp extension homologous to vector end) *GCTAGC* (*Nhe I*) ATT GAG CCG AGT GGG TTC AAG-3'. The PCR products were purified and directionally cloned between *Kpn I* and *Nhe I* sites in the promoterless Firefly luciferase reporter vector pGL4.10 [luc2] (Promega) using the In-Fusion® HD Cloning Kit (Clontech) as recommended by the supplier. Both reporter constructs were used after confirmation of their sequences (Eurofins Genomics). Plasmid DNA was prepared using the Qiagen Maxi Prep Kit (Qiagen).

2.5. Mutation of E-box-like elements in the 483-bp mTXNIP promoter reporter

Both E-box-like elements in the 484-bp 5′ flanking region of the *mTXNIP* gene were mutated at bp −364 to −359 (CACGAG to CACTAT) and −353 to −348 (CACGAG to CACTAT) using the QuickChange® Site-Directed Mutagenesis Kit (Agilent Technologies) according the manufacturer's instructions. The reporter construct was used after confirmation of its sequence (Eurofins Genomics). Plasmid DNA was prepared using the Qiagen Maxi Prep Kit (Qiagen).

2.6. Cell culture and transfection

HEK 293 cells were purchased from Sigma-Aldrich and cultured in Dulbecco's Modified Eagle's Medium supplemented with 10% (v/v) heat-inactivated FBS, 2 mM L-glutamine, 100 U/ml penicillin and 100 μg/ml streptomycin in a humidified atmosphere containing 5% CO_2 at 37 °C. HEK 293 cells were transiently transfected into 96-well plates (seeded at 2×10^4/well) using Lipofectamine® 3000 (Invitrogen) with a total of 100 ng of expression plasmids. The plasmid mix included 50 ng of firefly luciferase reporter plasmid where various constructs of the TXNIP promoter were cloned, 1 ng of pcDNA3.1-BMAL-1 or not and 1 ng of pcDNA3.1-CLOCK or not plus 25 ng of pKS vector as carrier and 25 ng of pGL4.74[*hRluc*/TK] vector (Promega) as *Renilla* luciferase normalization vector.

2.7. Luciferase assay

At 48 h post-transfection, luciferase activity was evaluated using the Dual-Glo® Luciferase Assay System (Promega) according to the manufacturer's instructions. Luminescence was measured on a luminometer FLUOstar OPTIMA (BMG LABTECH). For each sample, the data were normalized by dividing the firefly luciferase activity (expressed from the reporter vector) by the *Renilla* luciferase activity (expressed from the normalization vector).

2.8. Western blot analysis

Proteins were extracted from synchronized macrophages with the CelLytic™ M reagent (Sigma-Aldrich) containing a Protease Inhibitor Cocktail (Roche Diagnostics GmbH). Protein content was determined using the Pierce™ BCA Protein Assay Kit (Thermo-Scientific) as recommended by the supplier. Proteins (20 μg) were separated on AnykD™ Criterion™ TGX™ Precast Gels (Bio-Rad) and electro-transferred onto Immobilon®-P membranes (Millipore). The blocking was assessed with 5% non-fat milk in Tris-buffered saline with 0.1% Tween-20 (TBST) for 1 h at room temperature. The blots were then incubated overnight at 4 °C with a

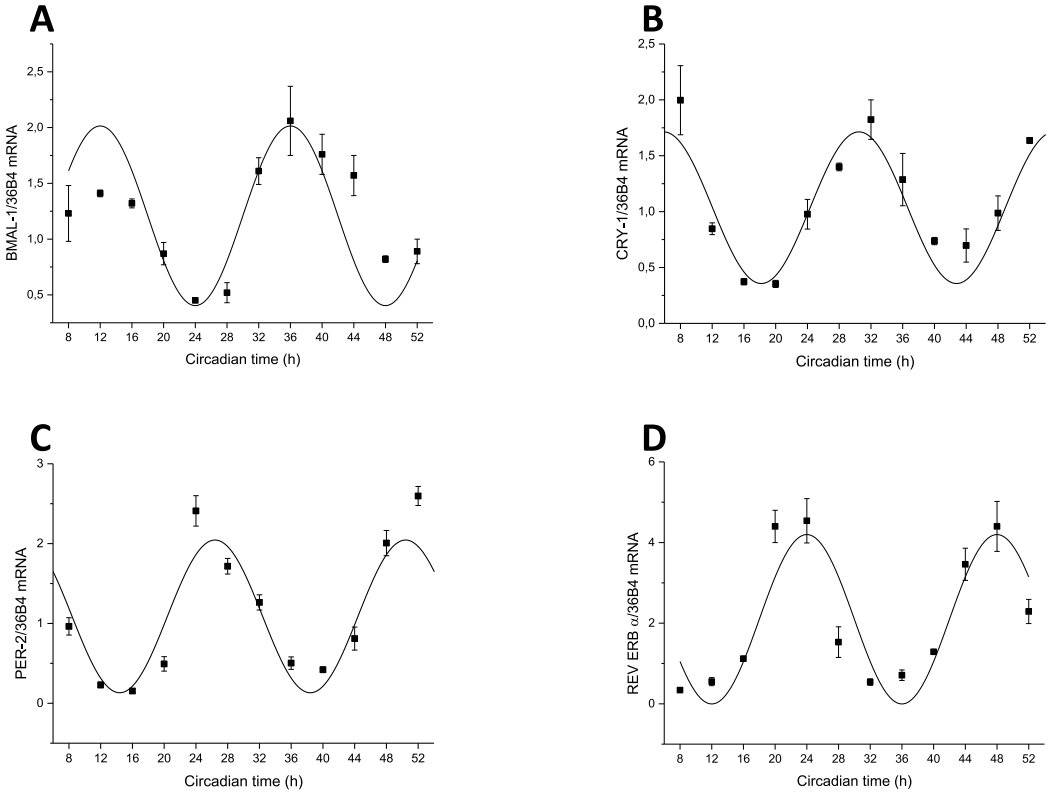

Fig. 1. Circadian rhythmicity of clock gene expression in synchronized murine peritoneal macrophages. Cells were synchronized by a 2 h shock with 100 nM DEX. Cells were harvested every 4 h for 52 h mRNA levels of four clock genes (*BMAL-1* (**A**), *CRY-1* (**B**), *PER-2* (**C**) and *REV ERB α* (**D**)) were evaluated by RT-qPolymerase Chain Reaction and normalized to *36B4*. Each value is the mean with SEM of three independent experiments. The curve represents the best fit obtained with the mathematical software *Origin 9.1*.

primary antibody against either Trx-1 (Abcam, 1:1000) Trx-2 (Invitrogen, 1:1000), TrxR1 (Abcam, 1:1000), TXNIP (Abcam, 1:1000). β-actin (Sigma-Aldrich, 1:5000) was used for normalization. The membranes were washed with TBST and probed with a horseradish peroxydase-conjugated secondary antibody for 1 h at room temperature. Membranes were revealed with the Clarity™ Western ECL Substrate (Bio-Rad) and the ChemiDoc™ MP Imaging System (Bio-Rad). The levels of protein expression were calculated as the relative band density with the ImageJ software.

2.9. Treatment of macrophage with MG-132, a proteasome inhibitor

After synchronization, murine peritoneal macrophages were treated with 5 μM MG-132 (Enzo Life Science). Proteins were then extracted from macrophages and Trx-1 expression was analyzed by Western blot as previously described.

2.10. Measurement of 4-hydroxynonenal (4-HNE) adducts

Synchronized macrophages were treated or not with anti-Trx-1-zymosan particles. Cells were washed and lysed in the CelLytic™ M reagent (Sigma-Aldrich) supplemented with a Protease Inhibitor Cocktail (Roche Diagnostics GmbH). The cell suspension was incubated for 15 min and centrifuged for 10 min at 10000×*g* at 4 °C. It was used to quantify HNE adducts with the OxiSelect™ HNE Adduct Competitive ELISA Kit (Cell Biolabs) according to the instructions of the supplier. The absorbance was read at 450 nm on a microplate reader (BioTek Instruments).

2.11. Measurement of TNF-α level

Culture medium of synchronized macrophages was collected, centrifuged for 15 min at 1000×*g* at 4 °C and used to assay TNF-α level with the ELISA MAX™ Deluxe Set Mouse TNF-α (BioLegend) according to the protocol described by the supplier. The absorbance was read at 450 and 570 nm on a microplate reader (BioTek Instruments).

2.12. Cellular cholesterol content

Culture medium of synchronized macrophages was collected, incubated with native LDL (100 μg/ml) for 4 h at 37 °C and then transferred on non-synchronized murine peritoneal macrophages for 48 h at 37 °C. Adherent cells were rinsed three times with PBS, lysed with PBS/0.1% Triton X-100 and sonicated for 5 s at 4 °C. Samples were diluted to 1.5 ml with distilled water and lipid extracted with chloroform/ethanol (4 ml; 1:1). Extraction was performed by vigorous agitation followed by centrifugation at 1500×*g* for 10 min at 4 °C. The upper phase was removed by aspiration and the lower phase (chloroform) evaporated under N_2. The dried lipids were dissolved in 200 μl cholesterol assay buffer of the kit. Total cholesterol was assayed with Total Cholesterol and Cholesteryl Ester Colorimetric Assay Kit II (BioVision) according to the instructions of the supplier. The absorbance was read at 450 nm on a microplate reader (BioTek Instruments).

2.13. Anti-Trx-1-zymosan preparation

Zymosan (Sigma-Aldrich) (100 mg) was suspended in PBS at

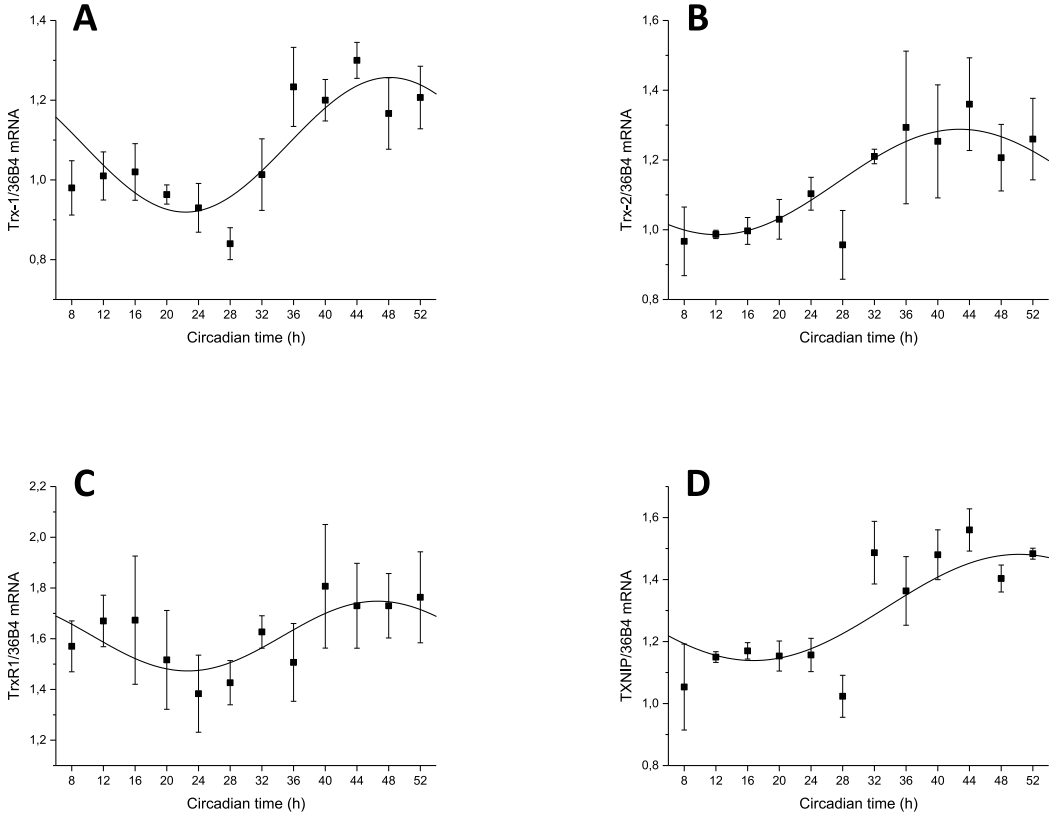

Fig. 2. Circadian rhythmicity of Trx-family gene expression in murine peritoneal synchronized macrophages. Cells were synchronized by a 2 h shock with 100 nM DEX. Cells were harvested every 4 h for 52 h mRNA levels of *Trx-1*, *Trx-2*, *TrxR1* and *TXNIP* genes were evaluated by RT-qPolymerase Chain Reaction and normalized to *36B4*. Each value is the mean with SEM of three independent experiments. The curve represents the best fit obtained with the mathematical software *Origin 9.1*.

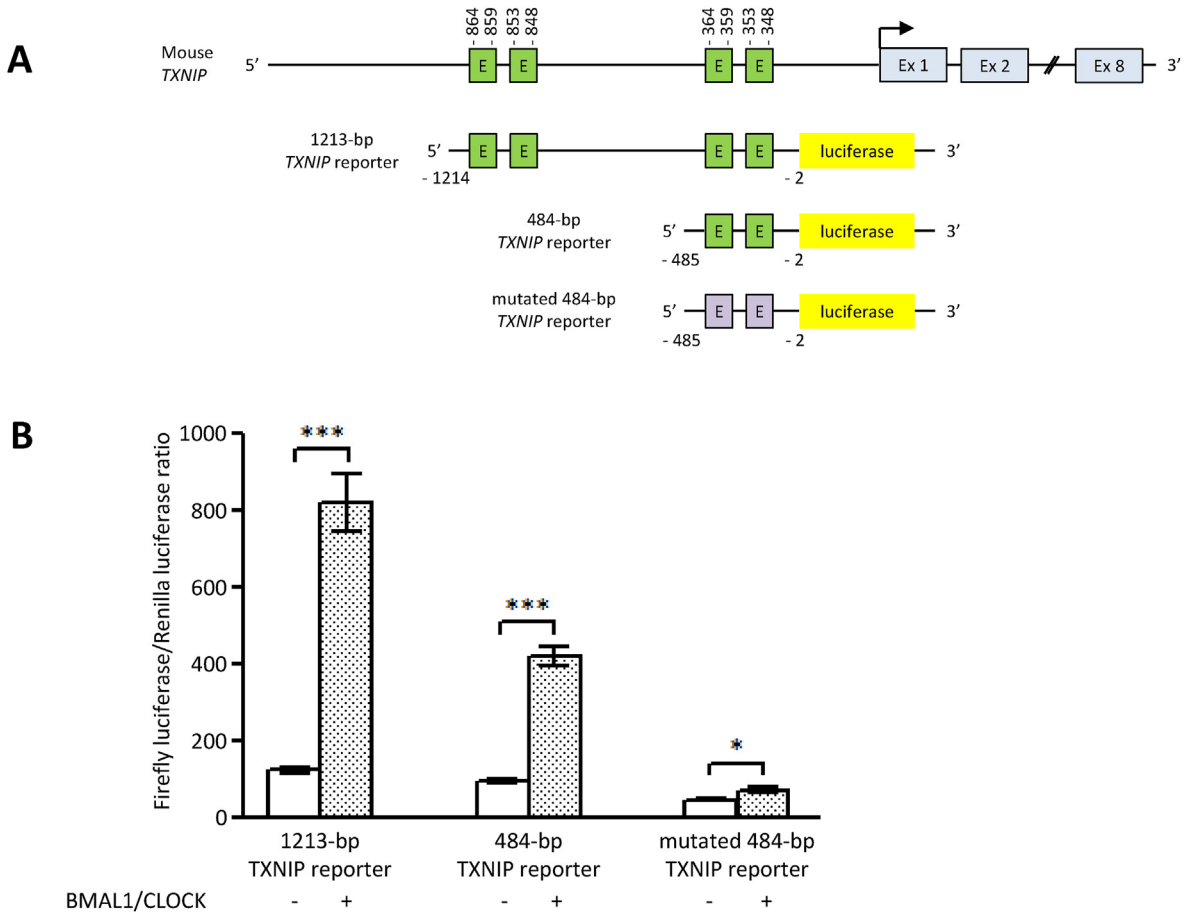

Fig. 3. Transcriptional regulation of the E-box-like elements in the *mTXNIP* promoter region by mBMAL-1/mCLOCK. A. Schematic representation of the mouse *TXNIP* gene and the three promoter regions cloned for luciferase assay. *Green boxes*, the location of the E-box-like elements in the promoter region; *purple boxes*, the mutated E-box-like elements. The arrow indicates the transcription start site. **B.** HEK 293 cells were co-transfected with one of the three constructs of *mTXNIP* promoter region together with pGL4.74[hRluc/TK] vector as control for the *Renilla* luciferase expression and (+) or not (−) with both mBMAL-1 and mCLOCK expression plasmids (1 ng each). Each value is the mean with SEM of three independent experiments, each performed in duplicate. Statistically significant differences, using the Mann-Whitney test, are indicated (*$p < 0.05$, ***$p < 0.001$).

10 mg/ml, heated for 60 min at 100 °C and subsequently centrifuged at 400×*g* for 5 min at room temperature. Zymosan was then suspended in 5 ml PBS/0.01% Tween 20 (PBST). To coat the zymosan particles with the antibody, 50 μl of the 20 mg/ml particle suspension were incubated with 100 μl of rabbit polyclonal anti-Trx-1 (Cayman Chemical) at 37 °C for 1 h. The particles were washed twice with PBST and suspended in 1 ml of serum free culture medium before introducing into the cell culture dish.

2.14. Mathematical modeling and statistical analyses

Results are presented as mean of three independent experiments ± SEM. All the fitting were performed by non-linear squares regression with the help of the mathematical software *Origin 9.1* (OriginLab, *Ritme Informatique*). The raw data for each curve were fitted to a sinus-derived damped wave function added to a linear drift term: $y = y_0 + A\sin\left(\pi\frac{x-x_c}{w}\right)$, with $A > 0$, $w > 0$ and $x > 0$ where y_0 represents the offset, A the amplitude, x_c the phase shift and w the half-period period. We removed the first two data points at t_{0h} and t_{4h} from the parameter estimation procedure as purely circadian variations may be perturbed by the DEX shock during the first hours.

Statistical significance was calculated with the Mann-Whitney test from the GraphPad Prism 5 software and was reported in the legend of each figure. Differences were considered statistically significant for values of $p < 0.05$.

3. Results

3.1. Circadian rhythmicity of clock gene expression in synchronized murine peritoneal macrophages

In this study, we first examined circadian gene expression in cultured murine peritoneal macrophages. Thus, following cell synchronization with DEX, total RNA and proteins were isolated from cells every 4 h and mRNA expression of BMAL-1, PER-1, PER-2, CRY-1, CRY-2, CLOCK and REV ERB α genes was determined. The synchronization was performed with DEX at 100 nM since synchronization with horse serum was reported to vary from one batch to another (personal communication, Prof. Francis Levy Laboratory, Villejuif, France). Thus, in a pilot experiment, DEX treatment did not enhance apoptosis, autophagy or necrosis on macrophages in comparison to horse serum synchronization (not shown). As shown in Fig. 1, BMAL-1, PER-2, CRY-1 and REV ERB α gene transcription exhibited a circadian expression with a robust oscillation while CRY-2, PER-1 and CLOCK genes exhibited also a circadian expression but with low oscillation (not shown).

3.2. Circadian rhythmicity of Trx-family gene expression in murine peritoneal synchronized macrophages

Next, we examined circadian gene expression at the mRNA levels of *Trx-1*, *Trx-2*, *TrxR1* and *TXNIP* (note that a circadian

expression should have a half-period (w) of ≈12 h). The results showed that none of these genes exhibited a circadian expression at the mRNA level (w = 25.8 ± 5.4 for Trx-1 (Fig. 2A), w = 30.6 ± 4.9 for Trx-2 (Fig. 2B), w = 23.9 ± 5.1 for TrxR1 (Fig. 2C) and w = 33.5 ± 8.6 for TXNIP (Fig. 2D)).

3.3. Transcriptional regulation of the E-box-like elements in the mTXNIP promoter region by mBMAL-1/mCLOCK

Since all the studied genes do not show a circadian expression at the mRNA level we analyzed their promoter region looking for E-box like elements. Indeed, it has been reported that, in mammals, CLOCK and BMAL-1 form a heterodimer and bind to CACGTG or CACGTT type E-box elements and activate not only the transcription of *PER* or *CRY* genes, but also many other genes, called clock controlled genes (CCGs). Interestingly, the analysis of the promoter region of the *TrxR1* gene showed the presence of E-boxes in agreement with a previously reported data [20]. In addition, a close examination of the TXNIP promoter sequence up to 1800 bp revealed the presence of two clusters, each consisting 2 E-box like elements separated by 5 base pairs: a proximal element located between −364/-348 bp and a distal element between −864/-848 bp. Since *TXNIP* gene does not possess a circadian expression at the mRNA level, we attempted to verify whether these E-box elements are nonfunctional. Because peritoneal macrophages are known to be difficult to transfect, we performed transfection assays in HEK 293 cells. The cells were transiently co-transfected with three constructs of the TXNIP promoter driven the luciferase gene reporter: -1214/-2 bp promoter containing the 4 E-boxes, a short promoter containing the only 2 proximal E-boxes and same construct with two mutated E-boxes (Fig. 3A). The HEK cells were co-transfected with a mix containing or not 1 ng of pcDNA3.1-BMAL1, 1 ng of pcDNA3.1-CLOCK, plus 25 ng of pRL-TK plasmid and 25 ng of pKS vector as a carrier. Interestingly, the results showed that cells transfected with the mixture containing the large fragment (−864/-848) express a high level of the luciferase activity in comparison to the control transfected cells (Fig. 3B). In addition, this luciferase activity is higher than the activity obtained with the short promoter fragment (−364/-348) (Fig. 3B). In contrast, the luciferase activity in transfected cells with the mutated fragment is comparable to the control cells (Fig. 3B).

3.4. Circadian rhythmicity of Trx family protein expression in murine peritoneal synchronized macrophages

Among the Trx system, only *Trx-1* and *TXNIP* genes exhibited a circadian expression at the protein level (w = 12.5 ± 0.8 for Trx-1 and w = 13.2 ± 1.5 for TXNIP) (Fig. 4 A and D) but not *Trx-2* and *TrxR1* genes (w = 27.9 ± 7.9 for Trx-2 and w = 21.6 ± 5.8 for TrxR1) (Fig. 4B and C). In addition, the rhythmicity of Trx-1 protein was found to be under the control of proteasome activity since inhibition of the proteasome significantly abolished such rhythmicity (Fig. 5).

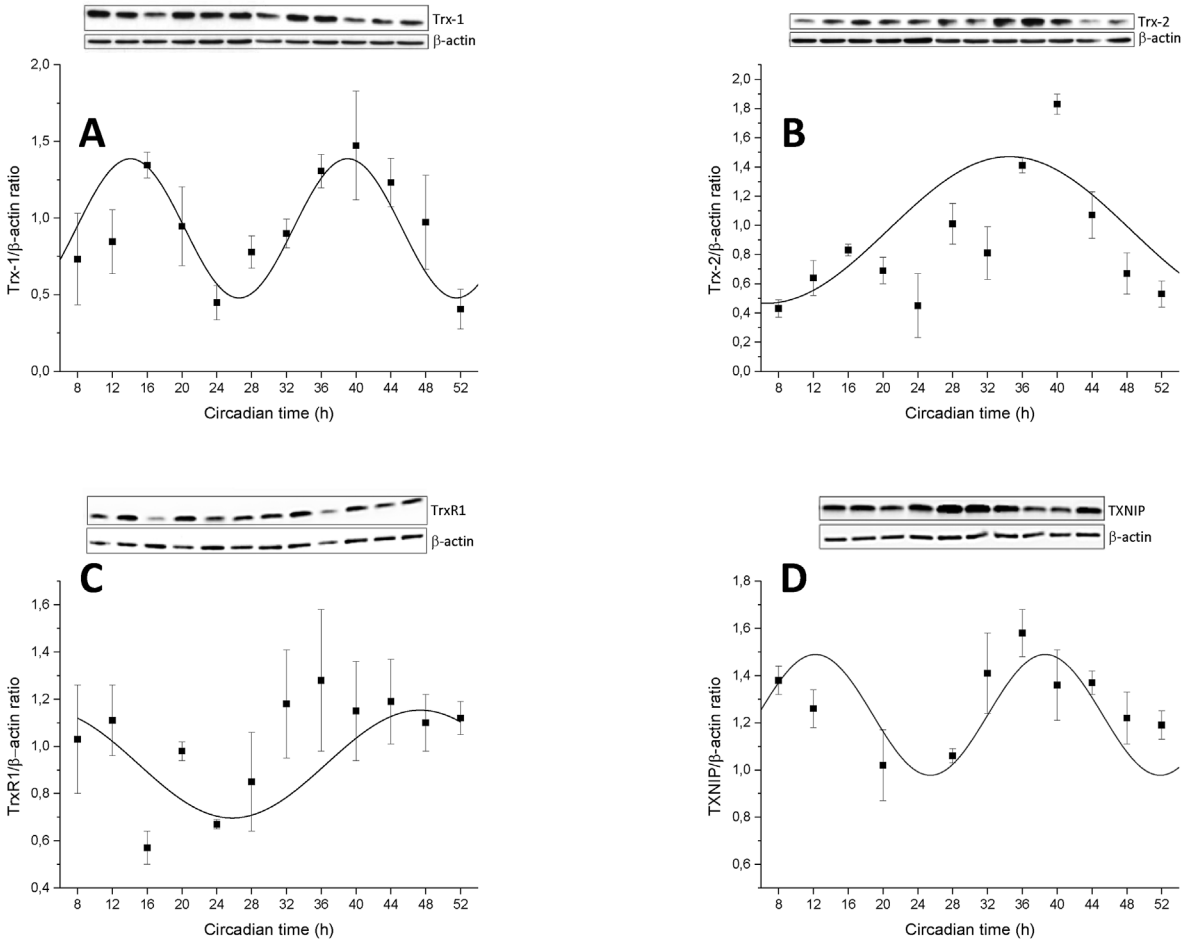

Fig. 4. Circadian rhythmicity of Trx family protein expression in murine peritoneal synchronized macrophages. Cells were synchronized by a 2 h shock with 100 nM DEX. Cells were harvested every 4 h for 52 h **A - D**. Whole-cell lysates were analyzed respectively for Trx-1 (**A**), Trx-2 (**B**), TrxR1 (**C**) and TXNIP (**D**) expression by Western immunoblotting using specific antibodies. β-actin was the loading control. Each value is the mean with SEM of three independent experiments. The curve represents the best fit obtained with the mathematical software *Origin 9.1*. A representative Western blot is shown for each Trx family protein.

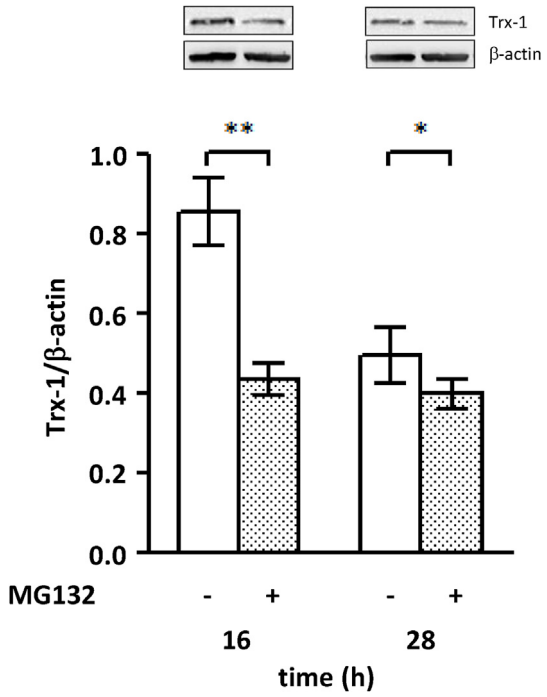

Fig. 5. Effect of proteasome inhibition on Trx-1 expression in murine peritoneal synchronized macrophages. Dexamethasone synchronized cells were treated either with 5 μM MG132 (+) or medium only (−). Cells were harvested 16 and 28 h after synchronization. Trx-1 expression in cell lysate was determined by Western immunoblotting; β-actin was the loading control. Western blots were quantified densitometrically and the results were presented as a graph. Each value is the mean with SEM of three independent experiments, each performed in duplicate. Statistically significant differences, using the Mann-Whitney test, are indicated (*$P < 0.05$, **$P < 0.01$). A representative Western blot is shown for each time.

3.5. A link between the Trx-1 expression and 4-HNE, TNF-a production and cholesterol accumulation in cultured macrophages

Next, a link was shown between the circadian rhythmicity of the Trx-1 and 4-HNE, an important marker of lipid oxidation (Fig. 6B); Trx-1 and TNF-α, an important marker of inflammation in atherosclerosis (Fig. 6C) and Trx-1 and the level of total cholesterol accumulated within macrophages, a hallmark of atheroma plaque (Fig. 6D). Indeed, when the protein of Trx-1 is expressed at a low level (Fig. 6A), the 4-HNE level is high (Fig. 6B). In contrast, when the level of Trx-1 is high (Fig. 6A), the 4-HNE level is low (Fig. 6B). In addition, when the Trx-1 is blocked by a specific neutralizing antibody, the level of 4-HNE increased suggesting a specific negative link between the Trx-1 and 4-HNE levels (16 h: 0.96 versus 2.37 μg/ml; 28 h: 1.35 versus 2.59 μg/ml) (Fig. 7). Again, when the Trx-1 is highly expressed (Fig. 6A), the level of TNF-α is low (Fig. 6C). In contrast, when the Trx-1 is expressed at a low level (Fig. 6A), the TNF-α level is high (Fig. 6C). In line with the above results, we reported a significant accumulation of total cholesterol in macrophages (Fig. 6D). Such lipid accumulation depends also on the rhythmicity of Trx-1. Indeed, when Trx-1 is highly expressed (Fig. 6A) the intracellular level of cholesterol is less (Fig. 6D) than when macrophages express a low level of Trx-1 suggesting that modulation of the oxidative stress by Trx-1 impacts on LDL oxidation and lipid accumulation.

4. Discussion

Disruption of circadian rhythms in rotating workers or frequent time zone travelers significantly increases the risk of several diseases including cardiovascular diseases [21]. These diseases are reported to be associated with elevated oxidative stress [22]. Since the Trx system, an important protective and antioxidant system in cardiovascular diseases, has been shown to be under circadian control in plants but not in mammals [12], therefore, we investigated whether it would exhibit circadian rhythmicity in synchronized cultured murine peritoneal macrophages, one of the principal cellular components in atherosclerosis development.

In this study, we demonstrated that murine peritoneal macrophages in culture possess the autonomous molecular clock machinery (Fig. 1). The expression patterns of the clock genes in these cells were similar to those in murine peritoneal macrophages isolated during the light or the dark period as well as to those in the SCN, liver and adipose tissue and other tissues [23–28]. Our results indicated that cultured peritoneal macrophages can be a good experimental model to study the circadian rhythmicity of the Trx system.

Using synchronized macrophages, we found that none of the Trx gene family possesses a circadian rhythmicity at the mRNA levels (Fig. 2) and this despite the presence, within the promoter regions, of an E-box sequence for *TrxR1* [20] and E-box like elements for *TXNIP* (this study). In contrast, promoters of *Trx-1* and *Trx-2* genes do not contain E-box elements. Of note, *in vitro* transfection revealed the functionality of the E-box like elements containing within the promoter region of *TXNIP* gene (Fig. 3). However, we observed a significant synchronized rhythmicity of Trx-1 and TXNIP at the protein level (Fig. 4 A and D) but not for Trx-2 and TrxR1 (Fig. 4 B and C). In addition, the rhythmicity of the Trx-1 at the protein level was found to be dependent of the proteasome activity (Fig. 5).

Taken together, our results indicate that all the *Trx* gene family does not exhibit the same regulation and that the presence of functional E-box elements in the *TXNIP* promoter is not sufficient to ensure circadian rhythmicity of this gene. Indeed, *in silico* analysis of the promoter regions of many antioxidant genes, such as *glutathione peroxidase-1*, *catalase*, *Superoxide dismutase-1*, and *TrxR1* reveals the presence of E-box elements in rodents and in humans indicating that these genes may be under direct transcriptional control of the BMAL-1/CLOCK complex [20]. Nevertheless, Rey, G et al. explored potential downstream target genes for BMAL-1 in mouse liver, and found none of the antioxidant genes was identified as direct targets for BMAL-1 [29]. Of note, the circadian clock affects the transcription regulation of genes with antioxidant and oxidative activities through various ways. Thus, certain genes can be directly controlled by BMAL-1/CLOCK, RORs and REVERBs while some other genes can be regulated by clock-controlled transcriptional factors such as nuclear factor erythroid-2-related factor-2 (Nrf-2). In addition, regulation can also take place *via* clock-controlled chromatin-modifying enzymes (reviewed in Ref. [30]). In the case of Nrf-2, the expression of antioxidant genes can be indirectly regulated through this transcription factor. Indeed, the Nrf-2 was found in the cytoplasm bound to Kelch-like ECH-associated protein 1 (Keap1). Once activation by oxidative stress, it is released from Keap1 and translocated to the nucleus where it associates with the musculoaponeurotic fibrosarcoma protein. This complex binds to the antioxidant response element (ARE) of many antioxidant enzymes and regulates their transcription. Among the antioxidant enzymes γ-glutamyl cysteine synthetase, GST, catalase [31,32] and Trx-1 (Reviewed in Ref. [33]) possess ARE motif. It has been reported that upregulation of many antioxidant and detoxification genes is impaired in the Nrf2-knockout mice [34]. Of note, the expression pattern of Nrf-2 was reported to exhibit circadian variations [35] suggesting that Nrf-2 might be involved in circadian variations of the above antioxidant genes including Trx-1. Nevertheless, in the present study, the expression pattern of Trx-1 at the

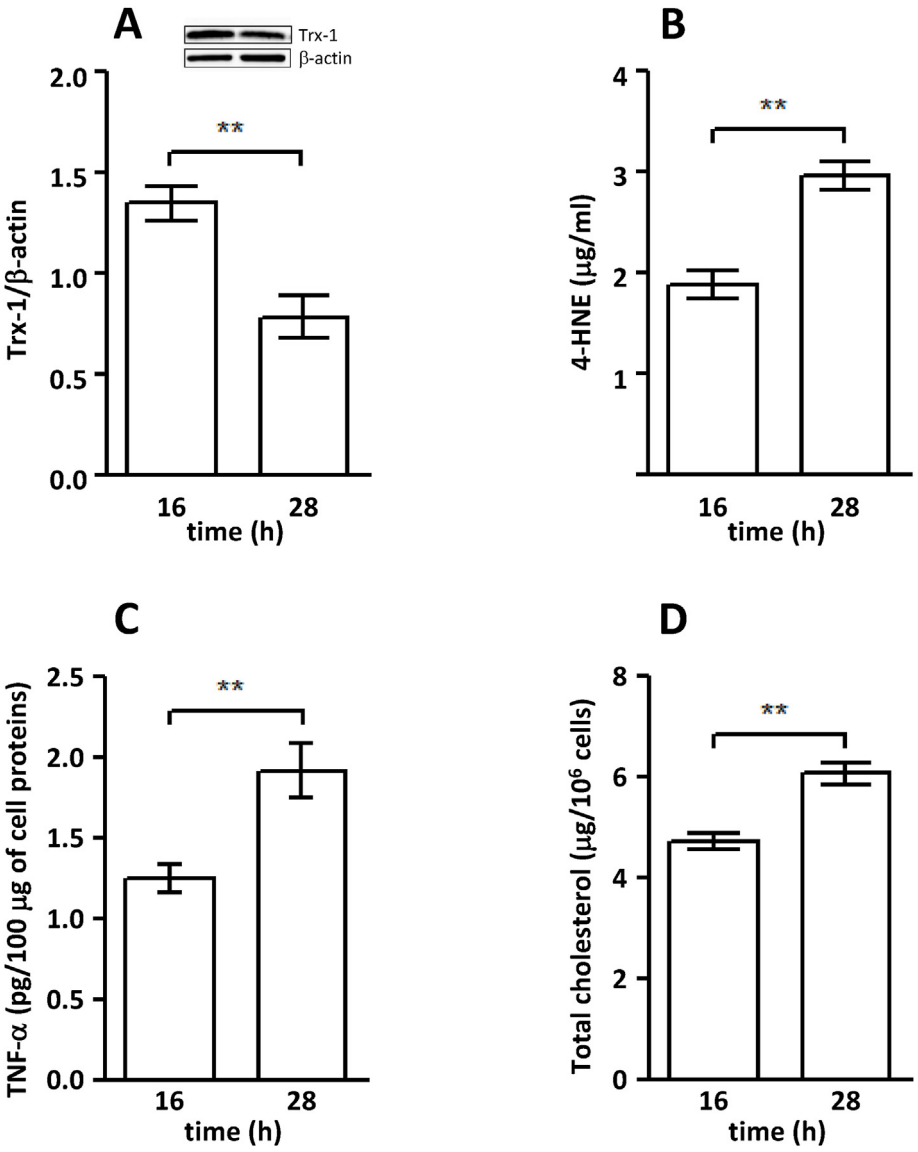

Fig. 6. Impact of the rhythmicity of the Trx-1 on different markers of atherosclerosis in murine peritoneal synchronized macrophages. Cells were synchronized by a 2 h shock with 100 nM DEX. Cells or culture media were harvested 16 and 28 h after synchronization. **A**. Trx-1 expression in cell lysate was determined by Western immunoblotting; β-actin was the loading control. **B**. 4-HNE adducts level in cell lysate was measured by ELISA. **C.** TNF-α level in culture media was quantified by ELISA. **D**. Total cholesterol accumulated within macrophages was determined enzymatically. Each value is the mean with SEM of three independent experiments, each performed in duplicate. Statistically significant differences, using the Mann-Whitney test, are indicated (**$P < 0.01$). A representative Western blot is shown for the Trx-1 expression at time 16 h and 28 h.

mRNA level does not follow circadian variations despite the presence of ARE within the Trx-1 promoter proving that the circadian rhythmicity of the Trx-1 expression is a complex mechanism. Indeed, it has been shown that DJ-1, a multi-functional protein with antioxidant and transcription regulatory activities, induces the expression of Trx-1 and DJ-1 knockdown in SH-SY5Y cells and DJ-1 deficiency in mice result in a decrease of the Trx-1 expression (protein and mRNA) [36]. Moreover, the ARE site of the Trx-1 promoter is necessary for DJ-1-dependent induction of Trx-1 expression [36]. Thus, Nrf-2, a critical inducer of ARE-mediated expression, is modulated by DJ-1 [36]. Overexpression of DJ-1 leads in increased Nrf-2 protein, stimulates its translocation into the nucleus and increased its recruitment onto the ARE site in the Trx-1 promoter [36]. Thus, the absence in our study of a circadian rhythmicity of the Trx-1, at the mRNA level, could be due to the absence of circadian rhythmicity of the DJ-1 protein. Further study is needed to clarify this mechanism.

A non-transcriptional mechanism of clock regulation of cellular redox balance was also observed [37,38]. In this study, inhibition of the proteasome activity abolished the rhythmicity of the Trx-1 at the protein level. However, the rhythmicity of the *TXNIP* gene is still not yet known. The proteasome system plays an central role in protein homeostasis [39]. A connection between the circadian clock, ROS production, antioxidant activities and elimination of oxidative modified proteins has been already reported [30,40] suggesting that elimination of oxidized modified proteins by the proteasome could also be regulated by the circadian clock. Interestingly, it has been reported that the transcription of various proteasome subunits is controlled by the circadian system [41,42]. In addition, it has been recently shown, in HEK 293 cells and human dermal fibroblasts, that the circadian accumulation of oxidized proteins and the modulation of proteasome activity could be explained, at least in part, by the circadian expression of both Nrf-2 and the proteasome activator PA28αβ [43]. Such a circadian control

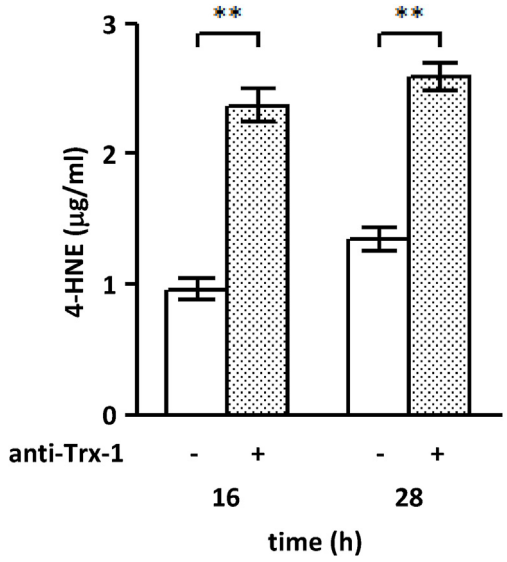

Fig. 7. Effect of blocking of the Trx-1 on the level of a lipid oxidation marker in murine peritoneal synchronized macrophages. DEX synchronized cells were treated with zymosan particles coated with an antibody anti-TRX-1. Cells were harvested 16 h and 28 h after synchronization. 4-HNE adducts in cell lysate was measured by ELISA. Each value is the mean with SEM of three independent experiments, each performed in duplicate. Statistically significant differences, using the Mann-Whitney test, are indicated (**$P < 0.01$).

of the Nrf-2/glutathione antioxidant system has been previously reported in the mouse lung and to play an important role in combating oxidative/fibrotic lung damage [44]. Of note, circadian cycles of post-translational oxidation of peroxiredoxin proteins have been reported in mouse liver [45] and in human red blood cells *in vitro* [38] while hyperoxidized peroxiredoxins have also been shown to be degraded by the proteasome. Hence, oxidative modifications such as carbonylation and nitrosylation could occur on Trx-1 and TXNIP leading to their degradation by the proteasome. Because the TXNIP can interact with Trx-1 to inhibit its activity, the degradation by proteasome of these proteins might occur either when they are forming a complex or in their free form.

Moreover, we reported a link between the circadian rhythmicity of the Trx-1 and certain important markers of lipid oxidation and inflammation such as 4-HNE, TNF-α, and the level of total cholesterol accumulated within macrophages. Indeed, it is well known that lipid peroxidation products accumulate, for example, with aging which is a risk factor for cardiovascular diseases [46–48]. This can happen because of the reduction in antioxidant defenses and the increase of oxidative stress [49–51]. Aldehydes such as 4-HNE, malondialdehyde and acrolein produced from the peroxidation of polyunsaturated fatty acids, form adducts on cellular proteins, resulting to a protein dysfunction with an impact in the pathophysiology of vascular aging [52]. Thus, we have shown a negative correlation between the Trx-1 and the 4-HNE levels in macrophages (Fig. 6 A and B). This result suggested a protection of lipids against oxidation by the Trx-1. Nevertheless, a double knockout model mouse such as ApoE$^{-/-}$/Trx-1$^{-/-}$ could help to clarify the impact of the absence of Trx-1 on atherosclerosis. Unfortunately, we could not generate such model since *Trx-1* gene deletion is lethal during mice embryonic development. Similarly, we showed a variation of the TNF-α level depending of the rhythmicity of the Trx-1 (Fig. 6C). In line with the above results, we reported a significant accumulation of total cholesterol in macrophages. Such lipid accumulation depends also with the rhythmicity of Trx-1 (Fig. 6D). This later finding is a surprising result since we expect a continuous accumulation at different degree depending of the presence of high or low level of oxLDL which is tightly linked to the high or low expression of Trx-1. Nevertheless, cholesterol accumulation within macrophages is a complex process and depends on the regulation of a variety of genes involved in cholesterol accumulation, (e.g. scavenger receptors genes), and cholesterol efflux (Apolipoprotein E and ATB-binding cassette superfamily receptors genes). In addition, intracellular proteins such as Acetyl Cholesterol Acyl Transferase (involving in cholesterol esterification), lipase (plays a role in cholesterol esterification hydrolysis) and lipid droplets associated proteins such as adipophilin and perilipin (play a role in lipid droplets protection against lipase hydrolysis) [53]. All these genes could also exhibit a circadian rhythmicity.

5. Conclusion

The circadian rhythm in frequency of occurrence of acute cardiovascular events has been documented [54]. Also, cardiovascular diseases were reported to be associated with elevated oxidative stress and antioxidant treatment can reduce the severity of these diseases in experimental models [22]. Since Trx-1 was reported to exert a variety of protective effects mainly through the control of oxidative stress but the increase of TXNIP prevents the beneficial activity of Trx-1 which results in more oxidative stress leading to more oxidized proteins and lipids as well as DNA damage. Hence, administration of Trx-1 at certain time point could be an interesting approach to overcome the TXNIP activity and to reduce oxidative stress, inflammation and lipid accumulation within the arterial wall.

Author contribution

Dominique Couchie: experimental design and performance; writing of the Materials and Methods section and the Figure legends; data analysis, design and production of the Figures. Tania Medali: experimental performance. Vimala Diderot: experimental performance. Michel Raymondjean: experimental design, data analysis and discussion. Bertrand Friguet: data analysis and discussion. Mustapha Rouis: design of the study and data analysis, discussion and writing of the manuscript.

Funding

The authors acknowledge funding from Sorbonne Université, CNRS and INSERM to UMR 8256 and U 1164, respectively.

Disclosure

All authors have approved the final article.

Declaration of competing interest

None.

Acknowledgments

The authors would like to thank Dr Kazuhiro Yagita from the Kyoto Prefectural University of Medicine, Kyoto, Japan for the generous gift of the expression plasmids containing the coding region of *mBMAL-1*, *mCLOCK* and *mDBP*; Dr Wilfried Le Goff from Sorbonne Université, INSERM, Institute of Cardiometabolism and Nutrition (ICAN), UMR_S1166, Paris, France for oxidized LDL preparation and the Fonds Marion Elizabeth Brancher for the financial support to Tania Médali.

References

[1] D. Steinberg, Low density lipoprotein oxidation and its pathological significance, J. Biol. Chem. 272 (1997) 20963–20966.
[2] C.K. Glass, J.L. Witztum, Atherosclerosis, the road ahead, Cell 104 (2001) 503–516.
[3] B.M. Freed, Y. Ouyang, J.M. McCue, Mechanisms of altered transcription by cigarette smoke, Toxicol. Sci. 59 (2001) 1–2.
[4] M.P. Antoch, R.V. Kondratov, Circadian proteins and genotoxic stress response, Circ. Res. 106 (2010) 68–78.
[5] C.K. Roberts, K.K. Sindhu, Oxidative stress and metabolic syndrome, Life Sci. 84 (2009) 705–712.
[6] A.P. Burke, A. Farb, G. Malcom, R. Virmani, Effect of menopause on plaque morphologic characteristics in coronary atherosclerosis, Am. Heart J. 141 (2001) S58–S62.
[7] M. Michalodimitrakis, A. Mavroforou, A.D. Giannoukas, Lessons learnt from the autopsies of 445 cases of sudden cardiac death in adults, Coron. Artery Dis. 16 (2005) 385–389.
[8] M.R. Ralph, R.G. Foster, F.C. Davis, M. Menaker, Transplanted suprachiasmatic nucleus determines circadian period, Science 247 (1990) 975–978.
[9] G. Ding, M. Fu, Q. Qin, W. Lewis, H.W. Kim, T. Fukai, M. Bacanamwo, Y.E. Chen, M.D. Schneider, D.J. Mangelsdorf, R.M. Evans, A. Yang, Cardiac peroxisome proliferator-activated receptor gamma is essential in protecting cardiomyocytes from oxidative damage, Cardiovasc. Res. 76 (2007) 269–279.
[10] J. Hirayama, P. Sassone-Corsi, Structural and functional features of transcription factors controlling the circadian clock, Curr. Opin. Genet. Dev. 15 (2005) 548–556.
[11] R. Hardeland, A. Coto-Montes, B. Poeggeler, Circadian rhythms, oxidative stress, and antioxidative defense mechanisms, Chronobiol. Int. 20 (2003) 921–962.
[12] S.D. Lemaire, M. Miginiac-Maslow, J.P. Jacquot, Plant thioredoxin gene expression: control by light, circadian clock, and heavy metals, Methods Enzymol. 347 (2002) 412–421.
[13] E.S. Arner, A. Holmgren, Physiological functions of thioredoxin and thioredoxin reductase, Eur. J. Biochem. 267 (2000) 6102–6109.
[14] C. Fu, C. Wu, T. Liu, T. Ago, P. Zhai, J. Sadoshima, H. Li, Elucidation of thioredoxin target protein networks in mouse, Mol. Cell. Proteomics 8 (2009) 1674–1687.
[15] S. Matsushima, D. Zablocki, J. Sadoshima, Application of recombinant thioredoxin1 for treatment of heart isease, J. Mol. Cell. Cardiol. 51 (2009) 570–573.
[16] J. Nordberg, an E.S. Arner, Reactive oxygen species, antioxidants, and the mammalian thioredoxin system, Free Radic. Biol. Med. 31 (2001) 1287–1312.
[17] S. Gromer, S. Urig, K. Becker, The thioredoxin system–from science to clinic, Med. Res. Rev. 24 (2004) 40–89.
[18] N. Maulik, D.K. Das, Emerging potential of thioredoxin and thioredoxin interacting proteins in various disease conditions, Biochim. Biophys. Acta 1780 (2008) 1368–1382.
[19] G. Spyrou, E. Enmark, A. Miranda-Vizuete, J. Gustafsson, Cloning and expression of a novel mammalian thioredoxin, J. Biol. Chem. 272 (1997) 2936–2941.
[20] R.V. Kondratov, O. Vykhovanets, A.A. Kondratova, M.P. Antoch, Antioxidant N-acetyl-L-cysteine ameliorates symptoms of premature aging associated with the deficiency of the circadian protein BMAL1, Aging (N Y) 1 (2009) 979–987.
[21] A.M. Curtis, G.A. Fitzgerald, Central and peripheral clocks in cardiovascular and metabolic function, Ann. Med. 38 (2006) 552–559.
[22] C.B. Anea, B. Cheng, S. Sharma, S. Kumar, R.W. Caldwell, L. Yao, M.I. Ali, A.M. Merloiu, D.W. Stepp, S.M. Black, D.J. Fulton, R.D. Rudic, Increased superoxide and endothelial NO synthase uncoupling in blood vessels of Bmal1-knockout mice, Circ. Res. 111 (2012) 1157–1165.
[23] M. Hayashi, S. Shimba, M. Tezuka, Characterization of the molecular clock in mouse peritoneal macrophages, Biol. Pharm. Bull. 30 (2007) 621–626.
[24] S.M. Reppert, D.R. Weaver, Molecular analysis of mammalian circadian rhythms, Annu. Rev. Physiol. 63 (2001) 647–676.
[25] S. Yamazaki, R. Numano, M. Abe, A. Hida, R. Takahashi, M. Ueda, G.D. Block, Y. akaki, M. Menaker, H. Tei, Resetting central and peripheral circadian oscillators in transgenic rats, Science 288 (2000) 682–685.
[26] K.F. Storch, O. Lipan, I. Leykin, N. Viswanathan, F.C. Davis, W.H. Wong, C.J. Weitz, Extensive and divergent circadian gene expression in liver and heart, Nature 417 (2002) 78–83.
[27] A. Balsalobre, S.A. Brown, L. Marcacci, F. Tronche, C. Kellendonk, H.M. Reichardt, G. Schutz, U. Schibler, Resetting of circadian time in peripheral tissues by glucocorticoid signaling, Science 289 (2000) 2344–2347.
[28] A. Arjona, D.K. Sarkar, Circadian oscillations of clock genes, cytolytic factors, and cytokines in rat NK cells, J. Immunol. 174 (2005) 7618–7624.
[29] G. Rey, F. Cesbron, J. Rougemont, H. Reinke, M. Brunner, F. Naef, Genome-wide and phase-specific DNA-binding rhythms of BMAL1 control circadian output functions in mouse liver, PLoS Biol. 9 (2011), e1000595.
[30] S.A. Patel, N.S. Velingkaar, R.V. Kondratov, Transcriptional control of antioxidant defense by the circadian clock, Antioxidants Redox Signal. 20 (2014) 2997–3006.
[31] T.W. Kensler, N. Wakabayashi, S. Biswal, Cell survival responses to environmental stresses via the Keap1-Nrf2-ARE pathway, Annu. Rev. Pharmacol. Toxicol. 47 (2007) 89–116.
[32] C.D. Klaassen, S.A. Reisman, Nrf2 the rescue: effects of the antioxidative/electrophilic response on the liver, Toxicol. Appl. Pharmacol. 244 (2010) 57–65.
[33] D.F. Mahmood, A. Abderrazak, K. El Hadri, T. Simmet, M. Rouis, The thioredoxin system as a therapeutic target in human health and disease, Antioxidants Redox Signal. 19 (2013) 1266–1303.
[34] K. Itoh, T. Chiba, S. Takahashi, T. Ishii, K. Igarashi, Y. Katoh, T. Oyake, N. Hayashi, K. Satoh, I. Hatayama, M. Yamamoto, Y. Nabeshima, An Nrf2/small Maf heterodimer mediates the induction of phase II detoxifying enzyme genes through antioxidant response elements, Biochem. Biophys. Res. Commun. 236 (1997) 313–322.
[35] Y.Q. Xu, D. Zhang, T. Jin, D.J. Cai, Q. Wu, Y. Lu, J. Liu, C.D. Klaassen, Diurnal variation of hepatic antioxidant gene expression in mice, PLoS One 7 (2012), e44237.
[36] J.Y. Im, K.W. Lee, J.M. Woo, E. Junn, M.M. Mouradian, DJ-1 induces thioredoxin 1 expression through the Nrf2 pathway, Hum. Mol. Genet. 21 (2012) 3013–3024.
[37] J.S. O'Neill, A.B. Reddy, Circadian clocks in human red blood cells, Nature 469 (2011) 498–503.
[38] J.S. O'Neill, G. van Ooijen, L.E. Dixon, C. Troein, F. Corellou, F.Y. Bouget, A.B. Reddy, A.J. Millar, Circadian rhythms persist without transcription in a eukaryote, Nature 469 (2011) 554–558.
[39] L. Borissenko, M. Groll, 20S proteasome and its inhibitors: crystallographic knowledge for drug development, Chem. Rev. 107 (2007) 687–717.
[40] N. Krishnan, A.J. Davis, J.M. Giebultowicz, Circadian regulation of response to oxidative stress in Drosophila melanogaster, Biochem. Biophys. Res. Commun. 374 (2008) 299–303.
[41] S. Panda, M.P. Antoch, B.H. Miller, A.I. Su, A.B. Schook, M. Straume, P.G. Schultz, S.A. Kay, J.S. Takahashi, J.B. Hogenesch, Coordinated transcription of key pathways in the mouse by the circadian clock, Cell 109 (2002) 307–320.
[42] R.A. Akhtar, A.B. Reddy, E.S. Maywood, J.D. Clayton, V.M. King, A.G. Smith, T.W. Gant, M.H. Hastings, C.P. Kyriacou, Circadian cycling of the mouse liver transcriptome, as revealed by cDNA microarray, is driven by the suprachiasmatic nucleus, Curr. Biol. 12 (2002) 540–550.
[43] A. Desvergne, N. Ugarte, S. Radjei, M. Gareil, I. Petropoulos, B. Friguet, Circadian modulation of proteasome activity and accumulation of oxidized protein in human embryonic kidney HEK 293 cells and primary dermal fibroblasts, Free Radic. Biol. Med. 94 (2016) 195–207.
[44] V. Pekovic-Vaughan, J. Gibbs, H. Yoshitane, N. Yang, D. Pathiranage, B. Guo, A. Sagami, K. Taguchi, D. Bechtold, A. Loudon, M. Yamamoto, J. Chan, G.T. van der Horst, Y. Fukada, Q.J. Meng, The circadian clock regulates rhythmic activation of the NRF2/glutathione-mediated antioxidant defense pathway to modulate pulmonary fibrosis, Genes Dev. 28 (2014) 548–560.
[45] A.B. Reddy, N.A. Karp, E.S. Maywood, E.A. Sage, M. Deery, J.S. O'Neill, G.K. Wong, J. Chesham, M. Odell, K.S. Lilley, C.P. Kyriacou, M.H. Hastings, Circadian orchestration of the hepatic proteome, Curr. Biol. 16 (2006) 1107–1115.
[46] L. Hayflick, How and why we age, Exp. Gerontol. 33 (1998) 639–653.
[47] R.A. Pruchno, M. Wilson-Genderson, M. Rose, F. Cartwright, Successful aging: early influences and contemporary characteristics, Gerontol. 50 (2010) 821–833.
[48] T. Flatt, A new definition of aging? Front. Genet. 3 (2012) 148.
[49] L. Rodriguez-Manas, M. El-Assar, S. Vallejo, P. Lopez-Doriga, J. Solis, R. Petidier, M. Montes, J. Nevado, M. Castro, C. Gomez-Guerrero, C. Peiro, C.F. Sanchez-Ferrer, Endothelial dysfunction in aged humans is related with oxidative stress and vascular inflammation, Aging Cell 8 (2009) 226–238.
[50] M.M. Bachschmid, S. Schildknecht, R. Matsui, R. Zee, D. Haeussler, R.A. Cohen, D. Pimental, B. Loo, Vascular aging: chronic oxidative stress and impairment of redox signaling-consequences for vascular homeostasis and disease, Ann. Med. 45 (2013) 17–36.
[51] M. El Assar, J. Angulo, L. Rodriguez-Manas, Oxidative stress and vascular inflammation in aging, Free Radic. Biol. Med. 65 (2013) 380–401.
[52] A. Negre-Salvayre, N. Auge, V. Ayala, H. Basaga, J. Boada, R. Brenke, S. Chapple, G. Cohen, J. Feher, T. Grune, G. Lengyel, G.E. Mann, R. Pamplona, G. Poli, M. Portero-Otin, Y. Riahi, R. Salvayre, S. Sasson, J. Serrano, O. Shamni, W. Siems, R.C. Siow, I. Wiswedel, K. Zarkovic, N. Zarkovic, Pathological aspects of lipid peroxidation, Free Radic. Res. 44 (2010) 1125–1171.
[53] G. Larigauderie, C. Furman, M. Jaye, C. Lasselin, C. Copin, J.C. Fruchart, G. Castro, M. Rouis, Adipophilin enhances lipid accumulation and prevents lipid efflux from THP-1 macrophages: potential role in atherogenesis, Arterioscler. Thromb. Vasc. Biol. 24 (2004) 504–510.
[54] A. Tanaka, T. Kawarabayashi, D. Fukuda, Y. Nishibori, T. Sakamoto, Y. Nishida, K. Shimada, J. Yoshikawa, Circadian variation of plaque rupture in acute myocardial infarction, Am. J. Cardiol. 93 (2004) 1–5.